

Numerical Modeling of Wave-Enhanced Turbulence in the Oceanic Upper Layer

LE NGOC LY* and ROLAND W. GARWOOD, Jr.

Department of Oceanography, Naval Postgraduate School, Monterey, CA 93943-5100, U.S.A.

(Received 28 June 1999; in revised form 31 January 2000; accepted 31 January 2000)

A coupled model of air-wave-sea interaction is modified based on a new roughness formulation and the latest data. The model parameters for aerodynamic roughness from below (ARB) and wave-dependent roughness from above (ARA, z_{0a}) are assumed equal. The combined roughness is assumed to be a function of friction velocity, gravity, air and seawater densities, and wave age (c_w). The model is used in a study of wave-enhanced turbulence under breaking waves to predict turbulent dissipation (ε), ARA, and drag coefficient (C_d). Both waves and shear production are considered as sources of ocean turbulent energy. The atmospheric part of the model is used only to specify a correct condition at the interface. Numerical experiments are performed to study the ε -distribution, z_{0a} and C_d , and to compare with data. The major achievement is model verification using all available data. The first full application of this model is in conjunction with an ocean circulation model in a coupled circulation-wave system. Simulations show that the ε -distribution is strongly dependent on local wind-forced wave heights. For each wind and wave state there is a particular wave-dependent depth that is verified by data. The comparison shows that the model predicted ε agrees well with the observed ε of the z^{-4} law distribution of Gargett (1989). Simulations also show that waves have an important role in causing ε to differ from the classical wall-layer theory and z_{0a} , with a value of 0.30 for the empirical constant a_a . The model-predicted ε , z_{0a} , C_d and C_{gd} agree well with data.

Keywords:

- Wave-turbulence,
- breaking wave effect,
- air-wave-sea coupling,
- turbulent dissipation,
- wave-dependent roughness.

1. Introduction

Breaking ocean waves are considered an important supplement to shear production of turbulent energy. Surface waves also play an important role in the velocity field of the ocean surface layer. The rate of turbulent energy dissipation per unit mass, ε , in the upper oceanic turbulent layer plays an important role in surface layer mixing, oceanic turbulent structure, and momentum and energy transport across the air-sea interface. It also plays an important role in gas and pollutant transfer across the interface. Distribution also has an important role in the verification of numerical models because, of all turbulence properties, only it can be measured readily in the ocean at the present time.

Numerous efforts have been made to observe ε in near surface layers (Benilov, 1973, 1991; Dillon *et al.*, 1981; Oakey and Elliott, 1982; Kitaigorodskii *et al.*, 1983; Shay and Gregg, 1984; Soloviev *et al.*, 1988; Gargett,

1989; Agrawal *et al.*, 1992; Drennan *et al.*, 1992; Osborn *et al.*, 1992; Moum *et al.*, 1995; Terray *et al.*, 1996). An excellent detailed review is given by Gargett (1989). Reviews of wave breaking and related subjects have appeared in recent years (Banner and Peregrine, 1993; Thorpe, 1995). A recent review of the role of surface-wave breaking in air-sea interaction is given by Melville (1996).

Here, our interest is in estimation of turbulent energy dissipation due to surface wave breaking. The reader whose primary interest is in the dynamics of wave breaking should refer to the above reviews. From the modeling point of view, we narrow our study to only numerical models that take surface waves into account using the turbulent closure schemes. Kundu (1980) and Klein and Coantic (1981) used turbulent kinetic energy (TKE) flux from the atmosphere to model the surface wave effect as a boundary condition in their ocean boundary layer models using turbulence closure schemes. Kundu (1980) used TKE flux in the form of mu_*^3 , with $m = 0.5$. Ly (1986, 1990, 1993) developed a coupled model taking into account the surface wave layer using a turbulence closure

* Corresponding author. E-mail: lely@nps.navy.mil

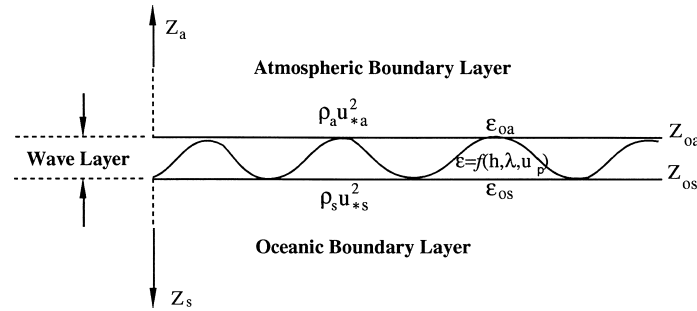


Fig. 1. The model domain showing the atmospheric and oceanic boundary layers with the wave layer. Here $\rho_a u_{*a}^2$ and $\rho_s u_{*s}^2$ are surface stresses; ϵ_{oa} and ϵ_{os} are turbulent energy dissipation rates which are a function of wave height (h), wave length (λ) and phase speed (u_p); z_{oa} and z_{os} are roughness lengths as seen from above/below, respectively.

scheme to study surface wave effects on dynamical and turbulent structures of the adjacent fluids. The wave layer was represented as a zone of mean and turbulent energy discontinuity between the atmosphere and ocean. The discontinuity was expressed in a form of $C_1 \rho_a u_{*a}^3$, where C_1 is a constant representing surface waves, and ρ_a is air density.

More recently, with the same approach as Kundu (1980) and Klein and Coantic (1981), Craig and Banner (1994) used a simple Ekman boundary layer model for the ocean with the 2.5 level turbulence closure scheme of Mellor and Yamada (1974, 1982) to study the wave-affected layer of the ocean. In their model (see also Craig, 1996), the action of breaking waves is represented by a TKE flux at the surface boundary condition in a form of αu_{*s}^3 with $\alpha = 100$ which was described as the wave energy factor (m in Kundu's model). They argued their model can accurately predict the $z^{-3.4}$ and $z^{-0.8}$ laws for the dissipation and velocity profile, respectively. The unresolved problems in their model are the wave energy factor $\alpha = 100$, and anomalous roughness length z_{oa} , which is specified equal to 0.1–8 m to provide rough agreement with Osborn's *et al.* (1992), and Anis and Moum's (1992) ϵ datasets (see also Melville, 1996). Recently, this model was also used by Terray *et al.* (1996) and Drennan *et al.* (1996) to interpret their dissipation data. In using Craig and Banner's model, Drennan *et al.* (1996) specified the roughness length to be 0.1–10 m with $\alpha = 100$. These extreme values for roughness lengths and wave energy factor may lead to a physical inconsistency between various physical characteristics of the oceanic and atmospheric boundary layers including wave-affected depth, turbulent and dynamical structures, drag coefficient, surface air and water velocities, roughness length, friction velocities, and wave parameters. Also the wave energy factor and anomalous roughness length were not based on strong physical argument.

It is noted that none of the above models were able

to relate surface waves to wave breaking conditions or to typical physical wave parameters such as wave length, height, period, and phase speed at the spectral peak, which are predicted by ocean wave models. Another problem for most of the above models is that it is doubtful that the mixing length vanishes at an ocean surface containing surface waves, as assumed for many mixing-length models. The error is incurred in the ocean surface layers, to a depth on the order of the wave height.

Traditionally in physical oceanography and marine meteorology, there has been only an aerodynamic roughness z_0 . This is the roughness for the air side of the interface. Hereafter, we will call this the aerodynamic roughness from above (ARA, z_{oa} in Fig. 1). There are many studies of the dependence of ARA on waves. More details and reviews can be found in Toba *et al.* (1990), Donelan *et al.* (1993), and Monbaliu (1994). The ARA and its closely related parameter, drag coefficient, are important in many applications. Realistic formulation of ARA is also very important in the development of coupled atmosphere-ocean models.

In coupled models, an aerodynamic roughness from below (ARB, z_{os} in Fig. 1) is usually introduced in writing boundary conditions for the ocean part of a coupled model. Not much is known about the ARB, in both observational and theoretical studies. Kondo (1976) assumed that ARA was equal to ARB, $z_{oa} = z_{os}$. Toba (1988) introduced ARB, z_{os} , and he assumed that $z_{os} = z_{oa}$. He also assumed that $z_{os} = a_1 z_{oa}$ where a_1 is a constant. Zilitinkevich *et al.* (1991) used an analogy of ARB with ARA. To determine ARB, Ly (1986, 1990, 1993) posed ARB as an analog to the ARA of Charnock (1955). Kitaigorodskii (1994) incorporated the effect of breaking waves in the parameterization of sea surface roughness from below, but there were neither numerical calculations nor comparison with observational data to verify the theory.

The aim of the present investigation is to numeri-

cally study and compare with available data wave-enhanced turbulence in terms of turbulent energy dissipation distribution, roughness length, and drag coefficient under breaking waves in the ocean surface layer using a modified version of a coupled model (Ly, 1995). The modified model is based on a new roughness length formulation and the latest data. In the model, the oceanic turbulence sources are considered to be related both to mean shear velocity and surface breaking waves. The ε is written as a linear combination of terms representing dissipation from mean flow and breaking waves. The ε from breaking waves is estimated by using observed data, similarity, semi-empirical turbulence theories, and the wave breaking condition. Then ε is expressed in terms of wave parameters. Wave-dependent ARA and ARB (Ly and Garwood, 1999) are used in the model. The atmospheric part of the coupled model is used only to specify a correct condition at the air-sea interface. In Section 2, a brief description of the model is presented. The numerical simulations of ε -distributions and comparisons with observations are given in Section 3. The summary and remarks are given in Section 4.

2. The Model

In this section, a brief description of the ocean part of a modified coupled model based on a new roughness length formulation and the latest observed data is presented. Details of the basic model are given by Ly (1995). Figure 1 shows the domain of the basic model including the atmospheric and oceanic boundary layers and the wave layer. The atmospheric part of the model is considered only to provide a correct boundary condition at the air-sea interface. Thus, the model equations for oceanic boundary layers include equations for momentum, TKE, dissipation rate ε , eddy viscosity or turbulent exchange coefficient, and stratification in the ocean.

Details about the E - ε turbulence closure, its applications to the atmospheric and oceanic boundary layers, and comparison with the length scale approach and available observed data are given by Ly (1991). The turbulence closure includes TKE, ε , and Kolmogorov equations with the breaking wave parameterization. The TKE equation for the ocean can be written as

$$\begin{aligned} \frac{\partial E}{\partial t} = & \alpha_1 \left(-\overline{u'w'} \frac{\partial U}{\partial z} - \overline{v'w'} \frac{\partial V}{\partial z} + \frac{\alpha_3}{\alpha_1} \frac{g}{\rho_0} \overline{w'\rho'} \right) \\ & - \alpha_4 \frac{\partial}{\partial z} \overline{E'w'} - \alpha_2 \varepsilon \end{aligned} \quad (1)$$

where ρ_0 is the reference value of seawater density, ρ .

The energy-dissipation equation for the ocean has the form

$$\begin{aligned} \frac{\partial \varepsilon}{\partial t} = & \beta_1 \frac{\varepsilon}{E} \left(-\overline{u'w'} \frac{\partial U}{\partial z} - \overline{v'w'} \frac{\partial V}{\partial z} + \frac{\beta_3}{\beta_1} \frac{g}{\rho_0} \overline{w'\rho'} \right) \\ & - \beta_4 \frac{\partial}{\partial z} \overline{\varepsilon'w'} - \beta_2 \frac{\varepsilon^2}{E}. \end{aligned} \quad (2)$$

The first two terms of the right-hand side (RHS) in (1) and (2) represent TKE generation by mean velocity shear (shear production), the next terms are the buoyancy flux and vertical turbulent transport, and the last term of the RHS represents dissipation.

The K -closure scheme used in (1) and (2) is

$$-\overline{u'w'} = K_m \frac{\partial U}{\partial z}; \quad -\overline{v'w'} = K_m \frac{\partial V}{\partial z}; \quad -\overline{w'\rho'} = K_{eh} \frac{\partial \rho}{\partial z} \quad (3)$$

$$-\overline{E'w'} = K_e \frac{\partial E}{\partial z}; \quad -\overline{\varepsilon'w'} = K_\varepsilon \frac{\partial \varepsilon}{\partial z} \quad (4)$$

where K_e is used in the E -equation and K_ε is used in the ε -equation. The eddy viscosity coefficients are calculated using the Prandtl-Kolmogorov equation,

$$K_m = \alpha_{e\varepsilon} E^2 / \varepsilon \quad (5)$$

with universal constant $\alpha_{e\varepsilon} = 0.046$ (Monin and Yaglom, 1971). The sets of constants α and β link the eddy coefficient for buoyancy and transport with the eddy viscosity coefficient for momentum as

$$K_{eh} = \alpha_3 K_m; \quad K_{eh} = \beta_3 K_m; \quad K_e = \alpha_4 K_m; \quad K_\varepsilon = \beta_4 K_m. \quad (6)$$

The constants α in the TKE equation have the values: $\alpha_1 = \alpha_3 = 1$, $\alpha_2 = 0.046$, $\alpha_4 = 0.73$. The β set have the values: $\beta_1 = 1.43$, $\beta_2 = 1.97$, $\beta_3 = 1.45$, $\beta_4 = 0.70$. Hereafter, subscript $i = a$ for atmospheric variables and $i = s$ for oceanic ones.

Buoyancy terms in TKE and ε equations are related to stratification of the atmosphere by nondimensional stratification parameters, which are expressed in terms of the Obukhov length of the atmospheric boundary layer. The stratification in the ocean is defined using the nondimensional Vaisala frequency, N_n^2 . In this study, only neutral stratification is considered.

It is assumed that the momentum fluxes are continuous across the air-sea interface,

$$\rho_a u_{*a}^2 = \rho u_{*s}^2 \quad (7)$$

where ρ_a is air density, z_{0a} and z_{0s} are ARA and ARB (see Fig. 1), and u_{*s} is friction velocity of the seawater. Thus,

the relation between friction velocities of the two fluids is

$$u_{*s} = \left(\frac{\rho_a}{\rho} \right)^{1/2} u_{*a}. \quad (8)$$

The surface boundary condition for the TKE is written in the traditional form for the air-sea interaction problem, which is expressed in terms of friction velocity of the fluid flow as

$$E(z)|_{z_{0s}} = \alpha_{e\varepsilon}^{-1/2} u_{*s}^2 \quad (9)$$

where $\alpha_{e\varepsilon}$ is a nondimensional constant identical to that in Eq. (5), and z_{0s} is ARB. This boundary conditions for TKE at the interface is provided by Eq. (1) based on the classical law-of-the-wall theory (shear production is in a balance with the TKE dissipation). Ly's (1986) numerical study showed that surface waves are a supplementary source of turbulence in the lower/upper parts of the atmosphere/ocean. It is obvious that breaking wave effects need to be taken into account in (9). There are no observations of TKE at present, and it is not clear how to parameterize breaking waves in terms of TKE. Hence, for simplicity, the classical boundary condition for TKE is used in the model. This TKE boundary condition needs to be improved in the future.

Most difficulties that arise in numerical modeling and the study of the physics of air-sea coupled problems are at the interface (the wave layer in our case) of the two fluids. Across the interface air and seawater densities differ by nearly three orders of magnitude. In general, boundary conditions at the interface need to be written not at the actual surface, but at aerodynamic roughness lengths away from the interface on both sides. Unlike the ARA in numerical modeling of marine and oceanic boundary layers, in general, in the air-sea coupled models, the ARA/ARB on both sides of the interface are internal variables of the air-sea system. The value of ARA in general marine atmospheric and oceanic models is a fixed constant value (Jenter and Madsen, 1989; Craig *et al.*, 1993; Craig and Banner, 1994; Craig, 1996) or prescribed by formula such as Charnock's (1955). In air-sea coupled models (Ly, 1991, 1995) the ARA and ARB are internal parameters of the air-sea system.

Taking turbulent transport into account, a boundary condition for ε at the surface has the form (Ly, 1991)

$$\varepsilon(z)|_{z_{0s}} = \frac{u_{*s}^3}{kz_{0s}} [q_1 + (1 - q_1) \exp(-q_2)] \quad (10)$$

where

$$q_1 = \beta_1/\beta_2; \quad q_2 = (\alpha_2^{1/2} \beta_2/k^2 \beta_4)^{1/2}. \quad (11)$$

Here, z_{0s} is the wave-dependent ARB calculated in the model by (23). More details about z_{0s} will be found in Section 3.

The boundary conditions at the bottom of oceanic boundary layer are such that the velocities tend toward a geostrophic current while the momentum flux, turbulence (TKE), and dissipation (ε) vanish.

Based on the concept that both breaking waves and shear production are sources of turbulent energy in the ocean surface turbulent layer (Ly, 1995) we generate an equation for turbulent dissipation rate:

$$\varepsilon(z)|_{z_{0s}} = \frac{u_{*s}^3}{kz_{0s}} [q_1 + (1 - q_1) \exp(-q_2)] + \gamma (u_p h)^3 / \lambda^4. \quad (12)$$

The first term on the right side is the dissipation (taking diffusion into account) from the mean flow, and the second term on the right side is the dissipation from the breaking waves. It is noted that in the case where surface breaking waves are not taken into account, Eq. (12) reduces to Eq. (10) and a situation described by Ly (1991) occurs. The constant γ is taken equal to 1.0 in this study.

Using a wave breaking condition from the linear theory (Longuet-Higgins, 1969) and dispersion relations for developed waves, (12) can be written in the form

$$\varepsilon(z)|_{z_{0s}} = \frac{u_{*s}^3}{kz_{0s}} [q_1 + (1 - q_1) \exp(-q_2)] + 2\gamma c_w g \frac{u_{*a}}{(4\pi)^4}. \quad (13)$$

Here, the wave age is defined as $c_w = u_p/u_{*a}$ with the phase speed at the frequency peak u_p . In general, the sea state is characterized by the wave spectrum, but the wave age, c_w is commonly used to characterize sea state. The wave age parameter measures the stage of development wind sea (sea state). "Young" wind sea refers to a sea state when waves have just been generated by wind, while "old" wind sea refers to a saturated sea state, for which the energy is steady in time. It is noted that a c_w of the order of 10 corresponds to young wind sea, and a c_w of the order of 25 corresponds to an old wind sea.

Then, dissipation can be written in terms of the friction velocity of air flow, u_{*a} , and wave ages as follows:

$$\varepsilon(z)|_{z_{0s}} = c_w g u_{*a} \left\{ \frac{(\rho_a / \rho)^{3/2}}{ka_a} [q_1 + (1 - q_1) \exp(-q_2)] + \frac{2\gamma}{(4\pi)^4} \right\} \quad (14)$$

where a_a is a constant (see Eq. (18), below). Equation (14) can be written in a nondimensional form which is used in the computing process as

$$\begin{aligned} & \varepsilon_n(z_n)|_{z_{0ns}} \\ &= \left\{ \frac{1}{z_{0ns}} [q_1 + (1 - q_1) \exp(-q_2)] + \gamma \left(\frac{\rho_a}{\rho} \right)^{5/2} \left(\frac{g}{2\pi L f^2} \right)^4 \frac{k^9 h_n^3}{c_w^5} \right\} \end{aligned} \quad (15)$$

where $\varepsilon_n = k^2 \mathcal{E} / (f u_{*s}^2)$, h_n is nondimensional wave height ($h_n = h/L$), z_{0ns} is defined by (21), and $L = k u_{*s} / f$ is the typical depth scale for the Ekman layer in the ocean with the Coriolis parameter, f . The subscript “ n ” indicates any quantity in nondimensional form, while other variables are defined above. Equation (15) is a boundary condition at the air-sea interface for the ε -budget equation. This boundary condition for ε is expressed in terms of wave height and roughness length.

3. Wave-Dependent Aerodynamic Roughness Lengths, Drag Coefficients

At the interface, Ly (1986) assumed that the ARA and ARB are functions of u_{*i} , g , ρ_a , ρ . Following this procedure for wave-dependent ARA and ARB, we assume that the ARA/ARB are functions of $f(u_{*i}, g, \rho_a, \rho, c_w)$. Based on dimensional analysis and considering the ARA/ARB are inversely proportional to wave age (ARA is larger for young waves than for developed waves; see Donelan *et al.*, 1993; Kitaigorodskii, 1994), the following formula for the roughness of both sides (ARA and ARB) of the wave layer (see Fig. 1) is derived.

$$z_{0i} = a_i \left(\frac{\rho_a}{\rho} \right) \frac{u_{*i}^3}{g u_p} \quad (16)$$

where the functions $a_i(\rho_a/\rho)$ may be taken as empirical constants (Ly, 1986). Then, Eq. (16) can be rewritten as

$$z_{0i} = a_i \frac{u_{*i}^2}{g c_w}. \quad (17)$$

For generality, we have two values of a_i (a_a and a_s) for the ARA and ARB. Smith *et al.* (1992) found the empirical constant a_a equal to 0.48, based on the HEXOS (Humidity Exchange over the Sea experiment) dataset. The ARA/ARB in Eq. (17) have a general form with the functions a_i , and they also provide a functional dependence for ARB, which is very helpful in coupled modeling. It is important to note that while there is consensus agreement

on the importance of sea state on drag coefficient, the manner in which it exerts this influence is far from clear (Toba and Jones, 1992; Donelan *et al.*, 1993, 1995; Jones and Toba, 1995).

There is a strong disagreement between interpretation of datasets and investigators on how wind-induced waves affect the roughness length from above. Therefore modelers have difficulty choosing a roughness length. In this study, Eq. (17) is used mainly because it shows a clear decrease of the ARA (normalized by u_{*a}) with wave ages as most investigators (including Jones and Toba, 1995) have shown from their data. Another reason is to compare observational data for ARA and drag coefficients with the model output.

We adopt the nondimensional quantities as follow:

$$z_{ni} = f z_i / (k u_{*i}) = z_i / L_i \quad (18)$$

where L_i are typical depth scales for Ekman layers in the atmosphere and ocean. Applying (18) to (17), we have nondimensional roughness in the form:

$$z_{0ni} = a_i f \frac{u_{*i}}{g c_w}. \quad (19)$$

Using (7) and an expression for the geostrophic drag coefficient, C_{gd} in Eq. (25), Eq. (19) can be written for nondimensional roughness from above and below as

$$z_{0na} = a_a f \frac{C_{gd} U_{ga}}{g c_w} \quad (20)$$

$$z_{0ns} = a_s f \frac{C_{gd} U_{ga}}{g c_w} \frac{1}{28}. \quad (21)$$

In the dimensional form, we have

$$z_{0a} = \frac{k a_a}{g} \frac{C_{gd} U_{ga} u_{*a}}{c_w} \quad (22)$$

$$z_{0s} = \frac{k a_s}{g} \frac{C_{gd} U_{ga} u_{*a}}{c_w} \left(\frac{1}{28} \right)^2. \quad (23)$$

If we assume the ARA and ARB to be equal as did Kondo (1976), from (22) and (23) we have $a_s = (28)^2 a_a$. This assumption is used in the present study. Equations (20)–(23) are used as working equations for roughness lengths in the study. It is also important to note that our ARA and ARB are internal air-sea system parameters that depend on friction velocities of both fluids (see Ly, 1996 for more details).

Beside roughness length, the momentum fluxes are commonly estimated from a drag coefficient C_d , which is another way to express the surface roughness. The C_d is the neutral drag coefficient at 10 m height, which is calculated in the model as

$$C_d = \left(\frac{u_{*a}}{U_{10}} \right)^2 = (kU_{ga}C_{gd})^2 / U_{10}^2 \quad (24)$$

where U_{10} is wind speed at 10 m height provided by model equations for the wind profile. The geostrophic drag coefficient (C_{gd}) shows the relationship between wind stress and geostrophic wind or wind at the top of the atmospheric boundary layer (Ly, 1995):

$$\begin{aligned} (C_{gd})^2 &= \left(\frac{u_{*a}}{kU_{ga}} \right)^2 \\ &= (1 - 2m_0 \cos \hat{\beta} + m_0^2) \\ &\quad \cdot \left[(d_{z_{na}} \phi_{na} + C_\rho d_{z_{ns}} \phi_{ns})^2 + (d_{z_{na}} \varphi_{na} + C_\rho d_{z_{ns}} \varphi_{ns})^2 \right]^{-1} \end{aligned} \quad (25)$$

$$\begin{aligned} \tan \sigma_a \\ &= \left[m_0 (N_0 \sin \hat{\beta} + \cos \hat{\beta}) - 1 \right] \left[N_0 - m_0 (\cos \hat{\beta} - N_0 \sin \hat{\beta}) \right]^{-1} \end{aligned} \quad (26)$$

where

$$m_0 = \frac{U_{gs}}{U_{ga}} = 0.02; \quad \hat{\beta} - 360^\circ = \sigma_s - \sigma_a; \quad C_\rho = \left(\frac{\rho_a}{\rho} \right)^{1/2} \approx \frac{1}{28} \quad (27)$$

$$N_0 = (d_{z_{na}} \phi_{na} + C_\rho d_{z_{ns}} \phi_{ns}) (d_{z_{na}} \varphi_{na} + C_\rho d_{z_{ns}} \varphi_{ns})^{-1} \quad (28)$$

$$\begin{aligned} \phi_i &= -\overline{u_i' w_i'}; \quad \varphi_i = -\overline{v_i' w_i'}; \\ \phi_{ni} &= \frac{(-1)^{r+1} \phi_i}{u_{*i}^2}; \quad \varphi_{ni} = \frac{(-1)^{r+1} \varphi_i}{u_{*i}^2}. \end{aligned} \quad (29)$$

Here, r is equal to 1 for the atmospheric and 2 for oceanic variables; $\hat{\beta} = \pi/4$ is the angle between the geostrophic wind and geostrophic current (or wind/currents at the top/bottom of atmospheric and oceanic boundary layers).

The closed systems of nonlinear equations for the oceanic boundary layer and boundary conditions are solved in nondimensional form using the partly coupled algorithm of the matrix and simple pivotal condensation methods. In solving the system of equations for the ocean part of the coupled model, the atmospheric part is considered only to give a correct condition at the air-sea interface. The grid used for the simulations consists of 200 irregularly spaced points for the oceanic boundary layer. The domain of integration with the nondimensional depth, z_n , ranges from $0 \leq z_n \leq 2$. More details on the partly coupled numerical algorithm and computing schemes of the mathematical model are given by Ly (1996).

After obtaining numerical solutions of the air-wave-sea system, it is straight forward to calculate air-sea interaction characteristics including angles σ_a , σ_s (Eqs. (26) and (27)), angles between surface wind stress and geostrophic wind, and between surface and geostrophic currents).

4. Numerical Simulations

The numerical experiments are designed for various winds (wave heights) and wave ages to study the model aerodynamic roughness lengths, drag coefficients and the dissipation distributions in the upper turbulent layer of the ocean, and to compare them with observations. The coupled model is used for various cases of the aerodynamic roughness from above (ARA) with different values of the coefficient a_a in the study. Model roughness lengths from above (z_{0a}) and neutral drag coefficients (C_d) are presented and compared with available data. Our focus is also a study of the vertical distribution of ε in the oceanic turbulent layer with various winds, and its comparison with a typical dataset of z^{-4} distribution by Gargett (1989). The z^{-4} law for the ε vertical distribution in the ocean was believed to be evidence of the inadequacy of the constant-stress boundary-layer theory prediction. The model outputs and their comparisons with available data are shown in Figs. 2–6.

Figure 2 shows the dependence of nondimensional ARA on the inverse wave ages. The data from various sources are adapted from Donelan *et al.* (1993). The symbols show various field and laboratory datasets from Lake Ontario, HEXOS (Smith *et al.*, 1992), Atlantic Ocean, laboratories by Donelan (1990, wave tank), Keller *et al.* (1992, wave tank), and Toba *et al.* (1990). The lines with numbers are the model outputs using Eq. (17) with various values of the coefficient a_a . From the figure, it is seen that the line with coefficient of 0.3 best represents observational data of various sources. Then (17) will have a form:

$$z_{0a} = 0.30 \frac{u_{*a}^2}{g c_w}. \quad (30)$$

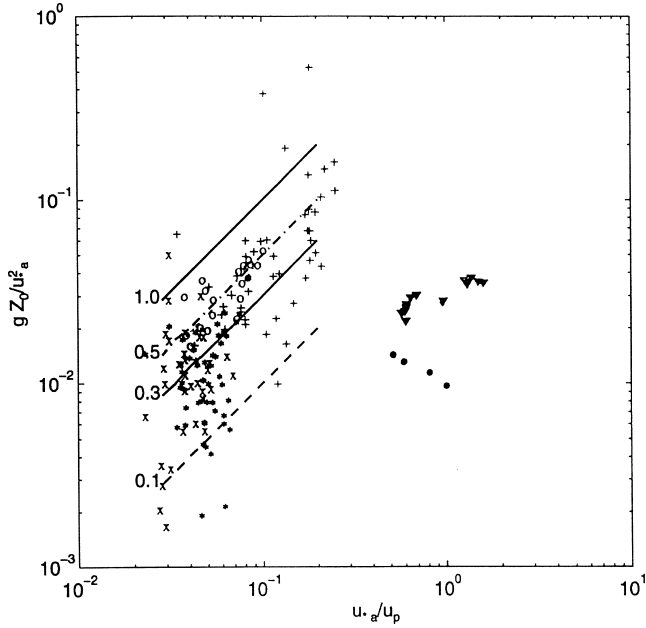


Fig. 2. Nondimensional roughness from above, gz_{0a}/u_{*a}^2 , versus inverse wave age u_{*a}/u_p . Data symbols (adopted from Donelan *et al.*, 1993): Lake Ontario +; HEXOS O; Atlantic Ocean, long fetch *; limited fetch x; Donelan (1990) water tank ∇; Keller *et al.* (1992) water tank ●. The lines with numbers are the model outputs with various values of the coefficient a_a in Eq. (26).

This ARA is used in the coupled model. Smith *et al.* (1992) found $a_a = 0.48$ is the best fit for their HEXOS dataset. In general, the roughness strongly depends on wave ages, and this dependence is quite linear. In Fig. 2, the young waves with $c_w = 5$ have $gz_{0a}/u_{*a}^2 = 0.06$, which are 6 times rougher than the developed waves with $c_w = 30$, which have $gz_{0a}/u_{*a}^2 = 0.01$. There may be a difference between field and laboratory data. Details about this matter are discussed by Jones and Toba (1995) and Donelan *et al.* (1995). Our ARA agrees better with field data (adapted from Donelan *et al.*, 1993) with long and unlimited fetches, because the model is for an open ocean. It is important to note that Toba *et al.* (1990) data in Fig. 2 should be used only in a consistent manner with their empirical equation for growing wind waves in local equilibrium with the wind (Toba *et al.*, 1990; Jones and Toba, 1995).

Vertical distribution of dissipation for various winds, U_{ga} , (winds at the top of the atmospheric boundary layer) equal to 11, 17, and 25 ms^{-1} are presented in Fig. 3. Figure 3 is plotted with the same scale as Fig. 4 (see below) to make comparison easier with observational data. As expected, the ϵ -distribution strongly depends on wave heights resulting from wind speed, U_{ga} . The wind increases by 55% from 11 ms^{-1} to 17 ms^{-1} , which corre-

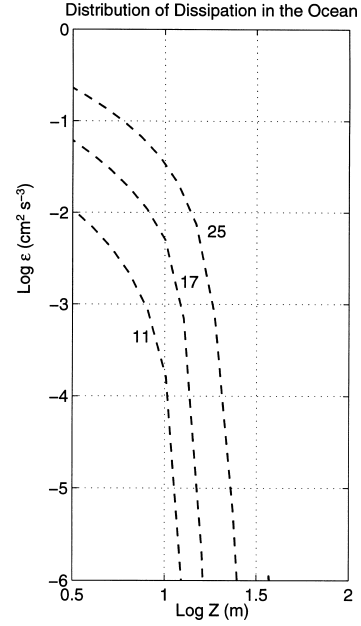


Fig. 3. Model simulations of dissipation profiles in the ocean at various winds (11, 17 and 25 ms^{-1}) and $c_w = 30$ in the ocean.

sponds to an increase in ϵ of about 20%. The numerical simulations (not shown here) confirmed that at the air-sea interface breaking wave-related dissipation dominates shear-related dissipation. The ratio of surface breaking wave-related dissipation to the total surface dissipation (shear-related and breaking wave-related) ranges from 65 to 75%. This ratio agrees well with the estimate by Kitaigorodskii (1973).

It is interesting to note that each wind (wave) generates a particular wave-affected depth. As wind (wave) increases, these depths increase 10% for wind increasing from 11 to 17 ms^{-1} , and 27% for wind increasing from 17 to 25 ms^{-1} . Comparing the dissipation-enhanced depths of winds 11 and 25 ms^{-1} (wave heights equal to 1.5 and 3.0 m, respectively, for our estimate), from Fig. 3 with a depth scale in Fig. 4 we can see the wave-affected depths can reach roughly to 15 to 30 m, respectively (stormy weather condition). These wave-affected depths agree with measurements by Kitaigorodskii *et al.* (1983) that showed a wave-affected region of about 10 times the wave amplitude. Thorpe (1984) suggested a wave-affected layer of depth approximately 0.2 of the surface wavelength. Osborn *et al.* (1992) used upward-looking acoustic instruments and shear probes mounted on a submarine in the Pacific Ocean and showed results qualitatively consistent with the results of Kitaigorodskii *et al.* (1983) and Thorpe (1984). The ϵ -distributions in Fig. 3 were calculated for $c_w = 30$.

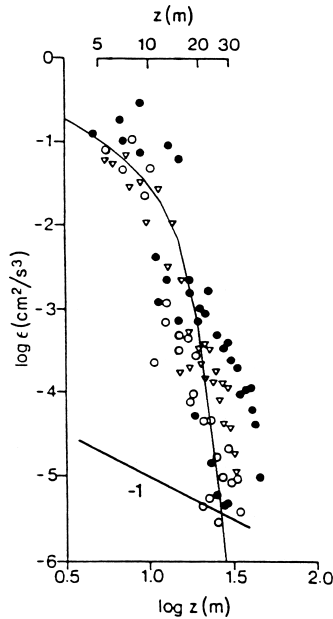


Fig. 4. Measurements of ε as a function of depth z in a shallow mixed layer in the northeast Pacific (Gargett, 1989). The line with “-1” shows the relationship $\varepsilon \sim z^{-1}$. Each point is a station average value (over 3–4 profiles within 20 min) of ε at depth z . Observations during intermittent stormy weather show ε varying approximately as z^{-4} , with little dependence upon the strength of wind forcing: strong (solid circles), $F_w \sim (2-3)U_{10} \text{ m}^{-3}$; ∇ medium, $F_w \sim 1U_{10} \text{ m}^{-3}$; weak (open circles), $F_w \sim (0.2-0.5)U_{10} \text{ m}^{-3}$. Here the energy flux is $F_w = \rho_a C_d U_{10}^3$ with wind U_{10} at a height of 10 m above the sea surface. The solid curve shows the model predicted ε -distribution.

Figure 4 is adapted from Gargett (1989). A curve of the model output from Fig. 3 is included. Figure 4 shows measurements of oceanic dissipation as a function of depth z in a shallow mixed layer in the northeast Pacific. Every point plotted is a station average of ε at depth z from 3–4 vertical profiles over a 15–20 minute period. The vertical resolution is ~ 2.5 m (see Gargett, 1989). Figure 4 shows observations during intermittently stormy weather for three classes of wind forcing (strong, medium, and weak). The observed ε profiles in the shallow (30–60 m) mixed layer consistently revealed a depth dependence closer to z^{-4} than z^{-1} . It is important to note that this ε -distribution was believed to be evidence of the inadequacy of the constant-stress boundary layer theory for the near-surface ocean (Gargett, 1989). The model predicted ε -distribution is a solid curve that is the same as the ε profile for the wind of 25 ms^{-1} in Fig. 3.

From Fig. 4, we can see that the model predicted ε profile agrees well with the observational ε profile of the z^{-4} law distribution by Gargett (1989) during intermit-

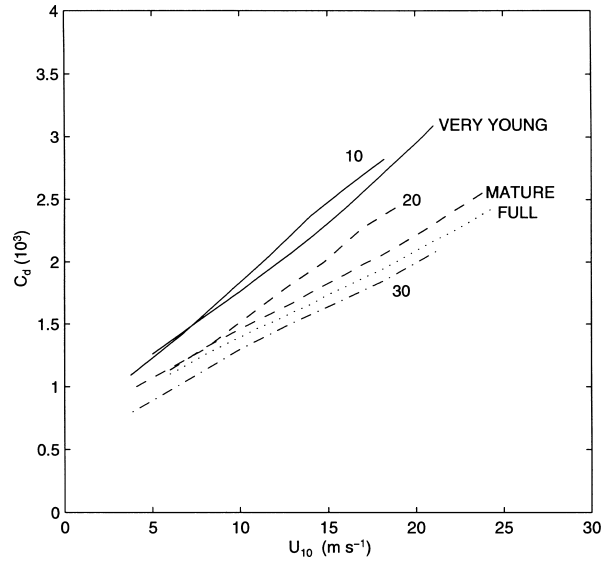


Fig. 5. Dependence of model drag coefficients on 10-m height winds and wave ages equal to 10, 20, and 30. Three other curves with “very young”, “mature” and “full” from observational data by Smith *et al.* (1992).

tently stormy weather. The z^{-4} law of ε -distribution is also obtained from observational data by Agrawal *et al.* (1992), Drennan *et al.* (1992), and Melville (1994) (see Section 1). Hopfinger and Toly (1976) also reported the z^{-4} law of dissipation distribution from their laboratory grid-mixing measurements (Thompson and Turner, 1975; Long, 1978). The TKE in the decaying grid-generated turbulence results from a balance between dissipation and diffusion (turbulent transport). In this case, the energy is supplied by the grid motion, and the breaking waves would be the source of the turbulence.

The solid line with “-1” in Fig. 4 shows the log law of the ε -distribution in the turbulent layer as $\varepsilon \sim z^{-1}$. This law of ε -distribution characterizing dissipation reverts to a simple wall layer scaling proportional to u_*^3 and inversely proportional to depth. This $\varepsilon \sim u_*^3 z^{-1}$ wall-layer law of ε -distribution is obtained if a log law of velocity distribution is considered in a scaling analysis of the oceanic ε -budget equation. The wall-layer law for the ε -distribution at the surface (roughness length) can be seen in Eq. (10), if the constant q_1 is taken equal to 1. In this case, Eq. (10) becomes the traditional boundary condition for ε at the surface with $\varepsilon(z_{0s}) = k^{-1} u_*^3 z_{0s}^{-1}$.

Our numerical results show that wind (waves) have an important role in driving the ε -distribution in the ocean away from a log law of the wall-layer theory. This can also be easily seen from Eq. (13). The first term of Eq. (13) with constant $q_1 = 1$ shows a log law of ε at the ocean surface. The second term shows a contribution from sur-

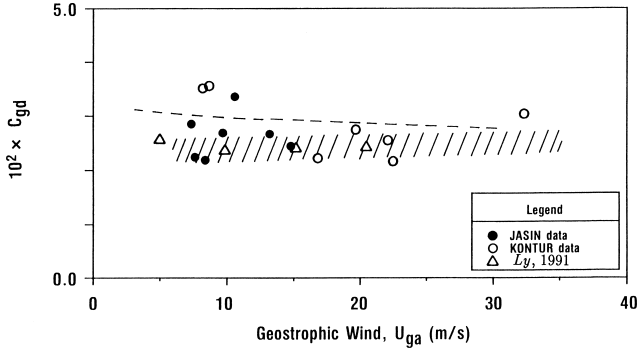


Fig. 6. The geostrophic aerodynamic drag coefficient, C_{gd} , as a function of winds (after Ly, 1991). The shaded area shows the range of values of C_{gd} by Grant and Whiteford (1987). Solid and open circles are JASIN and KONTUR data, respectively. The dashed line is this model C_{gd} for wave age $c_w = 30$.

face diffusion, which is an important TKE source under wave breaking conditions, and the third term shows a contribution from surface breaking waves. The numerical simulations also show that this model with the ARA (30) and parameter $\gamma = 1$ gives good agreement with the observed data.

The model drag coefficient, C_d , for the neutral atmospheric stratification as a function of wave age parameters 10, 20 and 30, and 10-m height winds is presented in Fig. 5. The figure shows that drag coefficient increases with wind speed and decreases for a larger wave age parameter. The C_d for the wave age equal to 30 is almost double the value at $U_{10} = 15 \text{ ms}^{-1}$ in comparison with that at 5 ms^{-1} . The model drag coefficients for a wave age equal to 10 have more than doubled their values at the same range of 10-m height winds. For the same $U_{10} = 15 \text{ ms}^{-1}$, C_d for the wave age of to 30 increases its value 63% for younger waves relative to wave age equal to 10. The model neutral drag coefficients for c_w , equal to 10, 20 and 30, are in a good agreement with observational data by Smith *et al.* (1992) for sea state varying from very young to mature and fully developed waves. The important feature of the model drag coefficient is that for the same 10 m height winds, C_d depends strongly on surface wind waves.

A comparison of observational and our model (dashed line) geostrophic drag coefficient, C_{gd} , is presented in Fig. 6. The C_{gd} is plotted against winds (after Grant and Whiteford, 1987; see also Ly, 1991). The shaded area shows the range of C_{gd} by Grant and Whiteford (1987) using observational data. The solid and open circles are JASIN and KONTUR data. Open triangles are Ly's (1991) model output. Wave conditions under which

the data were collected are not known. The simulations show that C_{gd} is not very sensitive to wave age and to the coefficient a_a of ARA. This also can be interpreted that C_{gd} is calculated by (25), in which c_w and ARA are not incorporated directly and ARA is considered as an internal model parameter. In general, the model produces geostrophic drag coefficients that are in a good agreement with observational data.

Overall, the simulations show that the model can predict well the ε -distribution, wave-dependent aerodynamical roughness length, and drag coefficient in comparisons with available observational data. The other model physical characteristics at the air-sea interface and of dynamical and turbulent structures of the air-sea system (not show here) are in a physically acceptable range. These are advantages of the air-wave-sea coupled model (Ly, 1995; Ly and Garwood, 1999) in comparison with a single fluid model of either air or sea (Melville, 1996).

5. Summary and Remarks

A numerical coupled model of air-wave-sea interaction is modified based on a new wave-dependent roughness length formulation and the latest available observations. The model is used in a numerical study of wave-enhanced turbulence under surface breaking wave conditions in terms of vertical distributions of turbulent dissipation, ε , wave-dependent roughness length, and drag coefficient. The study also focuses on comparison of the model output with available observations. In this model, breaking waves are considered to be another source of turbulent energy in the upper oceanic turbulent layer besides turbulent energy from shear-driven turbulence. The dissipation at the ocean surface is written in the form of a linear combination of terms representing shear-related dissipation and dissipation from breaking waves. The ε from breaking waves is estimated using similarity theory, observational data, and wave breaking conditions of linear theory. Thus, ε can be written in terms of wave parameters such as wave phase speed, height, and length which are expressed in terms of friction velocity. The above features have the advantage over other oceanic turbulent layer models of assuming surface turbulent kinetic energy fluxes result from breaking waves. The atmospheric part of the coupled model is considered only to give a realistic condition at the air-sea interface. Numerical experiments with various winds (wave heights) and wave ages were performed in the study.

In the ARA formulation, various values of the coefficient a_a that is a function $a(\rho_a/\rho)$ are used in the study. The numerical simulations confirm that the model nondimensional ARA, z_{0a} , normalized by friction velocity, u_{*a} , is strongly dependent on wave age. This normalized ARA is linear and better represents all available field datasets with a coefficient of 0.30 (Smith *et al.*, 1992

found 0.48 was the best fit for their HEXOS dataset). This normalized ARA cannot represent all available field and laboratory datasets by a curve (see Jones and Toba, 1995; Donelan *et al.*, 1995). It is important to note that both Donelan *et al.* and Toba *et al.* confirm that the younger waves are rougher than are the older waves. The model drag coefficient is strongly dependent on wave age and wind at 10 m. The geostrophic drag coefficient is not very sensitive to wave age or to the coefficient a_a of ARA.

The ε -distribution in the turbulent layer is strongly dependent on wave heights resulting from wind speed, U_{ga} . Each wind (wave) generates a particular wave-dependent depth. The comparison shows that the model predicted ε profile agrees well with the observed ε profile of the z^{-4} law distribution by Gargett (1989). The z^{-4} law of ε -distribution is also obtained from observational data by Agrawal *et al.* (1992), Drennan *et al.* (1992), Melville (1994), and from grid-mixing measurements by Hopfinger and Toly (1976). This z^{-4} law of ε -distribution was believed to be evidence of the inadequacy of the constant-stress boundary layer theory in ε prediction. Numerical simulations show that waves play an important role in driving ε -distribution in the turbulent layer away from a classical law of the wall-layer theory. The model output of the aerodynamical roughness lengths and wave-dependent drag coefficients also agree well with available observational data.

It is important to note that while the model ε -distribution agrees well with data, the model wave-dependent ARA, drag coefficient, and other physical characteristics such as boundary layer height/depth, ten-meter height wind (U_{10}), momentum fluxes, surface wind, currents, and turbulent structures (not show here) are in physically accepted ranges of understanding. These are the advantages of the air-wave-sea coupled model (Ly, 1995; Ly and Garwood, 1999) in comparison with all single fluid models (either air or sea) (e.g. Melville, 1996).

Overall, although the model can predict well the z^{-4} law of ε -distribution, there is a considerable scatter of various measurements of ε -distributions from a z^{-2} to a $z^{-4.6}$ law. Our model simulations show a strong dependence of ε -distribution on surface conditions (waves). The dependence of ε -distribution also on roughness length is obvious from the similarity scaling of the boundary condition. Then disagreements concerning the ε -distribution may result from various datasets being obtained under different surface waves.

Acknowledgements

The support of the Office of Naval Research under the grant N0001499WR30183 is gratefully acknowledged. The comments and suggestions of the reviewers and the editor (Dr. Ikeda) were very helpful and appreciated.

References

- Agrawal, Y. C., E. A. Terray, M. A. Donelan, P. A. Hwang, A. J. Williams, W. Drennan, K. K. Kahma and S. A. Kitaigorodskii (1992): Enhanced dissipation of kinetic energy beneath breaking waves. *Nature*, **359**, 219–220.
- Anis, A. and J. N. Moum (1992): The superradiant surface layer of the ocean during convection. *J. Phys. Oceanogr.*, **22**, 1221–1227.
- Banner, M. L. and D. H. Peregrine (1993): Wave breaking in deep water. *Annu. Rev. Fluid Mech.*, **25**, 337–397.
- Benilov, A. Yu. (1973): Generation of ocean turbulence by surface wave. *Atm. Ocean. Phys.*, **9**, 160–164.
- Benilov, A. Yu. (1991): *Turbulent Boundary Layers in the Ocean and Atmosphere in Interaction*. English trans. of Benilov's papers from *Izv. Acad. Nauk*. Stevens Institute of Technology, Hoboken, NJ, 284 pp.
- Charnock, H. (1955): Wind stress on a water surface. *Quart. J. Roy. Meteor. Soc.*, **81**, 639–640.
- Craig, P. D. (1996): Velocity profiles and surface roughness under breaking waves. *J. Geophys. Res.*, **101**, 1265–1277.
- Craig, P. D. and M. L. Banner (1994): Modeling wave-enhanced turbulence in the ocean surface layer. *J. Phys. Oceanogr.*, **24**, 2546–2559.
- Craig, P. D., J. R. Hunter and B. L. Johnston (1993): The implications of linearly varying eddy viscosity for wind-driven current profiles. *Cont. Shelf Res.*, **13**, 1–24.
- Dillon, T. M., J. G. Richman, C. G. Hansen and M. D. Pearson (1981): Near-surface turbulence measurements in a lake. *Nature*, **290**, 390–392.
- Donelan, M. A. (1990): Air-sea interaction. p. 239–292. In *The Sea*, ed. by B. LeMehaute and D. M. Hanes, J. Wiley & Sons.
- Donelan, M. A., F. W. Dobson, S. D. Smith and R. J. Anderson (1993): On the dependence of sea surface roughness on wave development. *J. Phys. Oceanogr.*, **23**, 2143–2149.
- Donelan, M. A., F. W. Dobson, S. D. Smith and R. J. Anderson (1995): Reply. *J. Phys. Oceanogr.*, **25**, 1908–1909.
- Drennan, W. M., K. K. Kahma, E. A. Terray, M. A. Donelan and S. A. Kitaigorodskii (1992): Observations of the enhancement of kinetic energy dissipation beneath breaking wind waves. p. 95–101. In *Breaking Waves*, ed. by M. L. Banner and R. H. J. Grimshaw, Springer, Berlin.
- Drennan, W. M., M. A. Donelan, E. A. Terray and K. B. Katsaros (1996): Oceanic turbulence dissipation measurements in SWADE. *J. Phys. Oceanogr.*, **26**, 808–815.
- Gargett, A. E. (1989): Ocean turbulence. *Annu. Rev. Fluid Mech.*, **21**, 419–451.
- Grant, A. L. M. and R. Whiteford (1987): Aircraft estimates of the geostrophic drag coefficient and Rossby similarity function A and B over the sea. *Boundary-Layer Meteorol.*, **39**, 219–231.
- Hopfinger, E. J. and J. A. Toly (1976): Spatially decaying turbulence and its relation to mixing across density interfaces. *J. Fluid Mech.*, **78**, 155–175.
- Jenter, H. L. and O. S. Madsen (1989): Bottom stress in wind-driven depth averaged coastal flows. *J. Phys. Oceanogr.*, **19**, 962–974.

- Jones, I. and Y. Toba (1995): Comments on 'The dependence of sea surface roughness on wave development'. *J. Phys. Oceanogr.*, **25**, 1905–1907.
- Keller, M. R., W. C. Keller and W. J. Plant (1992): A wave tank study of the determination of X-band cross sections on wind speed and water temperature. *J. Geophys. Res.*, **97**(C4), 5771–5792.
- Kitaigorodskii, S. A. (1973): *The Physics of Air-Sea Interaction*. Translated from Russian. Israel Program for Scientific Translations, 237 pp.
- Kitaigorodskii, S. A. (1994): A note on the influence of breaking wind waves on the aerodynamic roughness of the sea surface as seen from below. *Tellus*, **46A**, 681–685.
- Kitaigorodskii, S. A., M. A. Donelan, J. L. Lumley and E. A. Terray (1983): Wave-turbulence interaction in the upper ocean. Part II: statistical characteristics of wave and turbulent components of the random velocity field in the marine surface layer. *J. Phys. Oceanogr.*, **13**, 1988–1999.
- Klein P. and M. Coantic (1981): A numerical study of turbulent process in the marine upper layer. *J. Phys. Oceanogr.*, **11**, 849–863.
- Kondo, J. (1976): Parameterization of turbulent transport in the top meter of the ocean. *J. Phys. Oceanogr.*, **6**, 712–720.
- Kundu, K. P. (1980): A numerical investigation of mixed-layer dynamics. *J. Phys. Oceanogr.*, **10**, 220–236.
- Long, R. R. (1978): Theory of turbulence in a homogeneous fluid induced by an oscillating grid. *Phys. Fluids*, **21**, 1887–1888.
- Longuet-Higgins, M. S. (1969): On wave breaking and the equilibrium spectrum of wind-generated waves. *Proc. Roy. Soc. A.*, **310**, 151–159.
- Ly, L. N. (1986): Modeling the interaction between atmospheric and oceanic boundary layers, including a surface wave layer. *J. Phys. Oceanogr.*, **16**, 1430–1443.
- Ly, L. N. (1990): Numerical studies of the surface-wave effects on the upper turbulent layer in the ocean. *Tellus*, **42A**, 557–567.
- Ly, L. N. (1991): An application of the E - ϵ turbulence model to studying coupled air-sea boundary layer structure. *Boundary-Layer Meteorol.*, **54**, 327–346.
- Ly, L. N. (1993): On the effect of the angle between wind stress and wind velocity vectors on the aerodynamic drag coefficient at the air-sea interface. *J. Phys. Oceanogr.*, **23**, 159–163.
- Ly, L. N. (1995): A numerical coupled model for studying air-sea-wave interaction. *Phys. Fluids*, **7**(10), 2396–2406.
- Ly, L. N. (1996): A numerical algorithm for solving a coupled problem of the air-sea-wave interaction. *Mathematical and Computer Modelling.*, **24**, 7, 19–32.
- Ly, L. N. and R. W. Garwood, Jr. (1999): On breaking wave-enhanced turbulence in the oceanic surface boundary layer. *Proceedings. Thirteen Symposium on Boundary Layers and Turbulence*, AMS, Dallas, TX, January, p. 359–361.
- Mellor, G. L. and T. Yamada (1974): A hierarchy of turbulence closure models for planetary boundary layers. *J. Atmos. Sci.*, **31**, 1791–1806.
- Mellor, G. L. and T. Yamada (1982): Development of a turbulence closure model for geophysical fluid problems. *Rev. Geophys.*, **20**, 851–875.
- Melville, W. K. (1994): Energy dissipation by breaking waves. *J. Phys. Oceanogr.*, **24**, 2041–2049.
- Melville, W. K. (1996): The role of surface-wave breaking in air-sea interaction. *Annu. Rev. Fluid Mech.*, **28**, 279–321.
- Monbaliu, J. (1994): On the use of the Donelan wave spectral parameter as a measure for the roughness of wind waves. *Boundary-Layer Meteorol.*, **67**, 277–291.
- Monin, A. S. and A. M. Yaglom (1971): *Statistical Fluid Mechanics: Mechanisms of Turbulence*, MIT Press, Cambridge, 769 pp.
- Moum, J. N., M. C. Gregg, R. C. Lien and M. E. Carr (1995): Comparison of turbulence kinetic energy dissipation rate estimates from two ocean microstructure profilers. *J. Atmosph. Oceanic Tech.*, **12**, 346–366.
- Oakey, N. S. and J. A. Elliott (1982): Dissipation within the surface mixed layer. *J. Phys. Oceanogr.*, **12**, 171–185.
- Osborn, T., D. M. Farmer, S. Vagle, S. A. Thorpe and M. Cure (1992): Measurements of bubble plumes and turbulence from a submarine. *Atmosphere-Ocean*, **30**, 419–440.
- Shay, T. J. and M. C. Gregg (1984): Turbulence in an oceanic convective mixed layer. *Nature*, **310**, 282–285.
- Smith, S. D., R. J. Anderson, W. A. Oost, C. Kraan, N. Maat, J. DeCosmo, K. B. Katsaros, K. L. Davidson, K. Bumke, L. Hasse and H. M. Chadwick (1992): Sea surface wind stress and drag coefficients: The HEXOS results. *Boundary-Layer Meteorol.*, **60**, 109–142.
- Soloviev, A. V., N. V. Vershinsky and V. A. Bezverchnii (1988): Small-scale turbulence measurements in the thin surface layer of the ocean. *Deep-Sea Res.*, **35**, 1859–1874.
- Terray, E. A., M. A. Donelan, Y. C. Agrawal, W. M. Drennan, K. K. Kahma, A. J. Williams, III, P. A. Hwang and S. A. Kitaigorodskii (1996): Estimates of kinetic energy dissipation under breaking waves. *J. Phys. Oceanogr.*, **26**, 792–807.
- Thompson, S. M. and J. S. Turner (1975): Mixing across and interface due to turbulence generated by an oscillating grid. *J. Fluid Mech.*, **67**, 349–368.
- Thorpe, S. A. (1984): On the determination of K_p in the near-surface ocean from acoustic measurements of bubbles. *J. Phys. Oceanogr.*, **14**, 855–863.
- Thorpe, S. A. (1995): Dynamical processes of transfer at the sea surface. *Prog. Oceanogr.*, **35**, 315–352.
- Toba, Y. (1988): Similarity law of wind wave and the coupling process of the air and water turbulent boundary layers. *Fluid Dyn. Res.*, **2**, 263–279.
- Toba, Y. and I. S. F. Jones (1992): The influence of sea state on atmospheric drag. *EOS Trans. Amer. Geophys. Union*, **73**, 306.
- Toba, Y., N. Iida, H. Kawamura, N. Ebuchi and I. Jones (1990): Wave dependence of sea-surface wind stress. *J. Phys. Oceanogr.*, **20**, 705–721.
- Zilitinkevich, S. S., E. E. Fedorowich, S. D. Golosov, D. D. Kreiman, D. V. Mironov, M. V. Sabalova and A. Yu. Terzhevik (1991): Modeling air-lake interaction. *Physical Background*. Springer-Verlag, 129 pp.